RSC Advances

PAPER

View Article Online
View Journal | View Issue

Published on 16 September 2015. Downloaded by Michigan State University on 28/01/2016 09:27:12.

Cite this: *RSC Adv.*, 2015, **5**, 80357

# Biohybrid hematopoietic niche for expansion of hematopoietic stem/progenitor cells by using geometrically controlled fibrous layers†

Onon Batnyam,[a] Harue Shimizu,[a] Koichi Saito,[b] Tomohiko Ishida,[c] Shin-ichiro Suye[a] and Satoshi Fujita*[a]

Received 8th July 2015
Accepted 16th September 2015

DOI: 10.1039/c5ra13332g

www.rsc.org/advances

The expansion of hematopoietic stem/progenitor cells (HSPCs), which can give rise to all types of mature blood cells, is one of the actual challenges of regenerative medicine. In this study, we propose a construction of a 3D hematopoietic niche for the coculture of HSPCs and mesenchymal stem cells, which was prepared from geometrically controlled electrospun fibrous layers. The proliferation activity, retention of $CD34^+CD38^-$ immunophenotype and multipotency of the HSPCs in the artificial hematopoietic niche were analyzed by FACS and colony-forming unit assay. Results showed that the 3D biohybrid hematopoietic niche has a capacity to support self-renewal of HSPCs, maintaining their primitive phenotype and accommodate a large number of expanded cells. The geometry of the artificial niche served as a physical cue that controlled chemical signals to facilitate successful *in vitro* expansion and retention of HSPCs potential to differentiate into various lineages.

## Introduction

Nowadays, hematopoietic stem/progenitor cells (HSPCs) that have the properties of self-renewal and differentiation into all types of mature blood cells are becoming one of the essential tools in regenerative medicine.[1] The transplantation of HSPCs has become an important curative standard for hematological conditions such as multiple myeloma, non-Hodgkin's lymphoma, Hodgkin's lymphoma, β-thalassemia and sickle cell anemia.[2–4] These cells can be harvested from healthy donor's pelvis, femur, and sternum by bone marrow (BM) aspiration, but this method involves a high risk for the donor.[5–7] Next conventional source of HSPCs is peripheral blood (PB), but the cell collection procedure from this source is not easy and has a risk for a donor as well.[8] PB stem cells also have a high chance to cause graft-*versus*-host diseases, which is associated with lymphocyte subpopulation, particularly T-lymphocytes.[9] On the other hand, harvesting HSPCs from the umbilical cord blood (CB) has several advantages as source is readily available, involves a non-invasive collection procedure, and obtained cells are better tolerated across the human leukocyte antigens barrier. Moreover, the proliferative capacity of CB derived HSPCs (CB-HSPCs) is superior to that of cells from BM.[10] Unfortunately, HSPCs yield from a single donor CB is low, thus *in vitro* expansion of these cells is required to improve the clinical outcome of allogeneic HSPCs transplantation.

Previous studies have reported that *in vitro* 100-fold expansion of $CD34^+$ cells was obtained by culturing human $CD34^+CD38^-$ HSPCs with immobilized Notch ligand Delta-1,[11] and another study reported reprogramming of human endothelial cells with specific transcription factors such as FOSB, growth factor independent 1 (GFI1), RUNX1 and SPI1, combined with the signals from E4ORF1 endothelial cells led to induced HSPCs capable of engrafting to immunodeficient mice.[12] However, these methods are laborious and expensive. Other expansion methods involve utilization of coculture systems, where HSPCs seeded on top of mesenchymal stem cells (MSCs) monolayer.[13,14] In this system, the yield of expanded HSPCs is low and requires periodic subculturing as well as these conventional two-dimensional (2D) culture conditions are entirely different from the bone epiphyseal and metaphyseal regions, where homeostatic HSPCs are distributed.[15,16] Therefore, the high-yield *in vitro* expansion conditions of HSPCs should closely mimic a natural three-dimensional (3D) microenvironment, called hematopoietic niche, where the combination of soluble factors, intrinsic signaling pathways, adhesion molecules, local oxygen tension and cell-to-cell contact regulates the balance and homeostasis of HSPCs, self-renewal, proliferation and differentiation.[14,17–20] Many of those factors are facilitated by MSCs in hematopoietic niche or by their progeny committed to osteoblasts, which play an

[a]*Department of Frontier Fiber Technology and Science, Graduate School of Engineering, University of Fukui, Fukui, 910-8507, Japan. E-mail: fujitas@u-fukui.ac.jp*

[b]*Research Center for Regenerative Medicine, EIL Inc., Tokyo 174-0051, Japan*

[c]*Department of Obstetrics and Gynaecology, Itabashi Chuo Medical Center, Tokyo 174-0051, Japan*

† Electronic supplementary information (ESI) available. See DOI: 10.1039/c5ra13332g

Published on 16 September 2015. Downloaded by Michigan State University on 28/01/2016 09:27:12.

important role in nurturing of HSPCs in hematopoietic niche not only by supporting their proliferation, but also maintaining their primitive immunophenotype over a higher number of population doublings.[13,21] Another important aspect of hematopoietic niche is a 3D extracellular matrix (ECM) that provides mechanical support to all constituent of the niche. In our previous studies, we have unveiled a potential of electrospun fiber scaffolds geometry in controlling MSCs differentiation through mechanotransduction. In the presence of a mixed medium that facilitated both adipoinduction and osteoinduction, the adipoinduction was markedly inhibited on the fiber scaffolds with anisotropic properties supporting uniform osteogenesis,[22] which is essential for self-renewal and proliferation of HSPCs in hematopoietic niche.[21]

In this study, we have demonstrated a construction of 3D biohybrid hematopoietic niche-like microenvironment for the expansion of CB-HSPCs by fabricating high porous fiber scaffolds with different geometry and MSCs as feeder cells. The advantage of our niche is its beehive-like structure, where overlaid scaffolds can be easily separated from each other allowing convenient and efficient cell harvesting. The self-renewal, retention of $CD34^{+}CD38^{-}$ immunophenotype and multipotency of the HSPCs cultured in the artificial hematopoietic niches were evaluated by FACS and colony-forming unit assay. Our coculture system was designed to achieve efficient growth of HSPCs in high density by mimicking the microenvironment of hematopoietic niche in bone marrow endosteum.

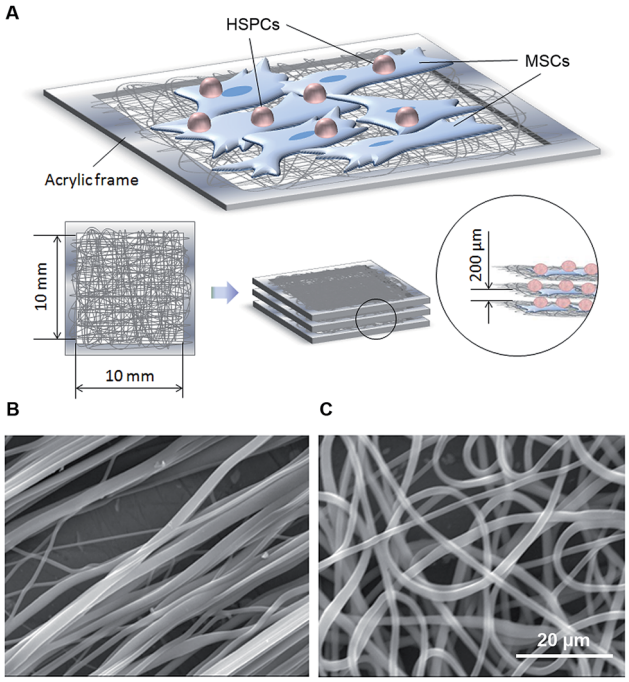


Fig. 1 (A) Schematic image of biohybrid hematopoietic niche. (B) SEM image of transversely isotropic Scaffold-I. (C) SEM image of anisotropic Scaffold-II.

## Material and methods

### Materials

Thermoplastic polyether–polyurethane–elastomer (PU, $M_w$ 146 000, Elastollan® 1180A10) was purchased from BASF (Ludwigshafen, Germany); tetrahydrofuran (THF), *N*,*N*-dimethylformamide (DMF), were purchased from Wako (Osaka, Japan). All other chemicals and reagents were of analytical grade and were used without further purification.

### Fabrication of electrospun fiber scaffolds

Electrospinning solution was prepared by dissolving PU in 95 v/v% THF and 5 v/v% DMF to obtain a final concentration of PU 12.5 wt/v%. PU nanofibers were electrospun onto acrylic frames with thickness of 200 μm (Fig. 1A) using a commercialized electrospinning setup (NANON-01A, MECC Co., Ltd, Fukuoka, Japan) which consisted of a closed chamber, high voltage power supply, a rotating collector ($\varphi$ 10 cm), a syringe pump, 5 mL syringe and a 27 G-needle. The applied voltage was set to 30 kV. The distance between the needle tip and collector was kept constant at 15 cm. The infusion rate of electrospinning solutions was controlled at 0.2 mL $h^{-1}$, the collector rotation velocity for transversely isotropic (Scaffold-I) and anisotropic fibers (Scaffold-II) were set at 1.5 m $s^{-1}$ and 0.05 m $s^{-1}$, respectively. To improve surface hydrophilicity of the fibers and sterilization, oxygen plasma treatment (40 kHz/100 W, 30 s, 0.1 MPa) was carried out by using a plasma reactor (Diener Electronics, Plasma Cleaner Femto, Ebhausen, Germany, chamber size, diameter 95 mm × depth 270 mm).

### Scanning electron microscopy

The morphological observations of obtained scaffolds were carried out using scanning electron microscope (SEM, Hitachi S-2600HS, Tokyo, Japan) at an accelerating voltage of 15 kV. Samples were sputtered with Pt/Pd using ion sputter (E-1030, Hitachi, Tokyo, Japan) for 120 s prior to observation. Images of ten randomly selected areas per sample were captured and used for fiber diameter and fiber orientation measurements using Fiji software (Fiji.sc; ImageJ 1.49m, NIH, USA). Fiber orientation was quantified using the second-order parameter, $S$, as follows:

$$S = (3\langle\cos^2\theta\rangle - 1)/2$$

where $\theta$ is an angle of each fiber and $\langle\cos^2\theta\rangle$ is the average of $\cos^2\theta$.[23,24]

### Isolation of hematopoietic stem cells from umbilical cord blood

Studies were approved by the institutional review board. CB was obtained from healthy donors with their informed consent. The $CD34^{+}$ cell fraction that is rich in HSPCs was isolated from fresh CB as follows; mononuclear cells were isolated by density gradient centrifugation using Lymphoprep (AXIS-SHIELD PoC AS, Oslo, Norway). After washing twice with Dulbecco's phosphate-buffered saline (PBS; Nissui Pharmaceutical Co. Ltd, Tokyo, Japan), $CD34^{+}$ cells were isolated by magnetic beads

 This journal is © The Royal Society of Chemistry 2015

Published on 16 September 2015. Downloaded by Michigan State University on 28/01/2016 09:27:12.

(Direct CD34 Progenitor Cell Isolation Kit; Miltenyi Biotech GmbH, Bergisch Gladbach, Germany) in accordance with the manufacturer's instructions. Isolated $CD34^+$ cells were cryopreserved using a bovine serum containing cell freezing media (Cellbanker, Nippon Zenyaku Kogyo Co., Ltd, Fukushima, Japan), and stored in liquid nitrogen until further use.

### Culture of human mesenchymal stem cells

Human bone marrow mesenchymal stem cells (MSCs, Takara Bio, Shiga, Japan) were cultured in Dulbecco's Modified Essential Medium (DMEM; Invitrogen, CA, USA) supplemented with 10% fetal bovine serum (FBS; Sigma-Aldrich, St. Louis, MO, USA), 100 U $mL^{-1}$ penicillin, and 100 μg $mL^{-1}$ streptomycin (Wako Pure Chemical Industries Ltd, Osaka, Japan). Cultures were incubated in a humidified atmosphere with 5% $CO_2$ at 37 °C. Cells were passaged upon reaching near confluency, and reseeded to a density of $3 \times 10^3$ cells per $cm^2$. Cells with passage numbers between 2 to 8 were used for further experiments.

### Coculture of hematopoietic stem cells with mesenchymal stem cells seeded on the layered fiber scaffolds

First, MSCs were seeded at a density of $2 \times 10^4$ cells per $cm^2$ onto prepared electrospun fiber scaffolds, which were washed twice with PBS and once with 10% FBS/DMEM prior cell seeding, and cultured at 37 °C for 1 week. Three replicates were carried out in each culture. Then, three layers of MSCs seeded fiber scaffolds were overlaid on each other in $2.5 \times 10^3$ cells per mL HSPCs and 2% methylcellulose (#400; Nacalai Tesque, Inc., Kyoto, Japan) containing PBS. Then cells were cocultured in StemPro-34 SFM (Invitrogen, CA, USA) serum-free medium specifically formulated to support the growth of human hematopoietic progenitor cells supplemented with 2 mM L-alanyl-L-glutamine (GLUTAMAX I; Invitrogen, CA, USA), 50 ng $mL^{-1}$ Flt-3 ligand, 50 ng $mL^{-1}$ stem cell factor, and 50 ng $mL^{-1}$ thrombopoietin (StemSpan CC110; Stemcell Technologies Inc., Vancouver, Canada). After 1 week of coculture at 37 °C under 5% $CO_2$ in a humidified atmosphere without changing the culture medium. The control cells were cocultured on monolayer of MSCs which were seeded in a $\varphi$ 35 mm culture dish. HSPCs cultured on Scaffold-I were named 3D culture-I (3D-I) and HSPCs cultured on Scaffold-II were named 3D-II (3D-II). Prior examinations cells were dissociated using 0.05% trypsin-EDTA solution (Wako Pure Chemical Industries Ltd, Osaka, Japan) and characterization by flow cytometry and colony-forming cell assay.

### Quantitative RT-PCR

Gene expression in feeder MSCs was analyzed by quantitative reverse transcription-polymerase chain reaction (qRT-PCR). Total RNA was extracted from MSCs using the High Pure RNA Isolation Kit (Roche Diagnostics, Mannheim, Germany), according to the manufacturer's instructions. RNA purity and concentration was quantified using NanoVue Plus spectrophotometer (GE Healthcare, Piscataway, NJ, USA). Complementary DNA (cDNA) was then synthesized from the extracted total RNA (1.6 μg) using the Transcriptor Universal cDNA Master kit (Roche). Specific cDNA was amplified by PCR using a reaction mix (20 μL) composed of 2 mM Tris–HCl (pH 8.0), 10 mM KCl, 0.01 mM EDTA, 0.1 mM DTT, 1 U DNA polymerase (TaKaRa Ex Taq; Takara Bio), 0.2 mM dNTP mixture, 0.5 μM of each primer, and approximately 100 ng of cDNA template. The synthesis conditions were as follows: 94 °C (45 s), 62 °C (30 s), and 72 °C (90 s). qRT-PCR was conducted using FastStart Essential DNA Green Master kit (Roche) and LightCycler® Nano instrument (Roche) in 15 μL of reaction mix with cDNA, and 5 μM each primer (*JAG1*: forward 5′-CGGGAACATACTGCCATGAAAATA-3′, reverse 5′-ATGCACTTGTAGGAGTTGACACCA-3′; *GAPDH*: forward 5′-CGTCTTCACCACCATGGAGA-3′, reverse 5′-CGGCCATCACGC CACAGTTT-3′). The amplification conditions were as follows: 95 °C (60 s) followed by 45 cycles of 95 °C (20 s), 60 °C (20 s), and 72 °C (20 s). The levels of PCR product were standardized to that of *GAPDH* mRNA, which was defined as 1 arbitrary unit.

### Flow cytometry

To analyze cell-surface expression of CD34 and CD38 marker proteins, HSPCs were labelled with anti-human CD34-FITC (clone 581, BD Pharmingen, CA, USA) and anti-human CD38-PE (clone HB7, Becton Dickinson and Co. CA, USA). In brief, collected cells were resuspended in 1% BSA/PBS, and incubated with fluorescence dye-conjugated antibodies (1 : 25 dilution) for 1 h at 4 °C. Then, cells were double stained with propidium iodide in order to exclude dead cells from the analysis and washed twice with 1% BSA/DPBS. For quantification of cell number 25 μL ($2.75 \times 10^4$ particles) of CountBright™ absolute counting beads (Invitrogen, CA, USA) were added to each sample immediately before counting. To reduce the noise of non-blood cells, the region of blood cells was determined by a FSC-SSC gating. The $CD34^+$ and $CD38^+$ quadrants were determined by reference to isotypic controls after compensation. Data acquisition and analysis was performed using FACSCalibur instrument (BD Biosciences, NJ, USA).

### Colony-forming units assay

Hematopoietic potency of the $CD34^+$ cells was examined by the colony-forming units (CFU) assay by resuspending the cells in a semi-solid methylcellulose medium (MethoCult GF H4434; StemCell Technologies, Vancouver, BC, Canada), which consisted from Iscove's modified Dulbecco's medium supplemented with 1% methylcellulose, 30% fetal bovine serum, 1% bovine serum albumin, 100 μM 2-mercaptoethanol, 2 mM L-glutamine, 50 ng $mL^{-1}$ stem cell factor, 10 ng $mL^{-1}$ GM-CSF, 10 ng $mL^{-1}$ IL-3 and 3 U $mL^{-1}$ erythropoietin and seeding at a density of $10^3$ cells per dish. Duplicates were performed in each culture. The cells were incubated in a humidified atmosphere with 5% $CO_2$ at 37 °C. At day 14 the number of CFU was counted based on the morphology of colonies as follows: burst-forming unit-erythroids (BFU-E), granulocytes/macrophages (CFU-GM), or granulocytes/erythroid/macrophages/megakaryocytes (CFU-GEMM). At day 28, the dense colonies larger than 1 mm in diameter were

Published on 16 September 2015. Downloaded by Michigan State University on 28/01/2016 09:27:12.

counted as high-proliferative potential colony-forming cells (HPP-CFC).

### Statistical analysis

All experiments were conducted at least three times, and all values were reported as the mean ± standard deviation (SD). Statistical analysis was carried out by Welch test using R commander (version 2.1-7).

## Results

### The 3D skeleton of an artificial niche and its function

In this study, for the *in vitro* expansion of HSPCs artificial hematopoietic niches were constructed. The skeleton of the constructs was composed of overlaid electrospun fiber scaffolds with different fiber orientations that were obtained *via* controlling the electrospinning collector rotation speed. The constructs composed of three overlaid transversely isotropic fibers were named Scaffold-I and constructs composed of three overlaid anisotropic fibers were named Scaffold-II (Table 1). For the fabrication of Scaffold-I and II with different geometrical features, PU that is highly elastic and biocompatible was used.

The diameter and orientation of fabricated fibers were analyzed from SEM images. Herein nanofibers composing both scaffold types did not show significant difference in their diameters, Scaffold-I = 1.72 ± 0.52 μm and Scaffold-II = 1.85 ± 0.5 μm. Fiber orientations were calculated by second-order parameter, $S$, where $S$ value closer to 1 referred to a perfectly aligned fibers and $S$ closer to 0 referred to a randomly oriented fibers. Second-order parameter measurement of Scaffold-I showed that nanofibers were aligned parallel ($S = 0.96 \pm 0.02$) conducing transversely isotropic properties (Fig. 1B). By contrast, in Scaffold-II, low rotational speed of the collector resulted in randomly oriented nanofibers ($S = 0.51 \pm 0.09$) resulting in anisotropic properties (Fig. 1C). SEM observations also showed that in the obtained scaffolds pores were interconnected and the average pore size of Scaffold-I and II were 32.8 ± 43.6 $\mu m^2$ and 8.6 ± 5.5 $\mu m^2$, respectively (Table 1). The average distance between each layer in both scaffolds was approximately 200 μm. These results show that we have obtained geometrically different scaffolds with uniformly interconnected pores.

### Gene expression in MSCs on biohybrid niches

To study the effect of scaffolds on the expression of *JAG1* in MSCs, which plays an important role in maintaining self-renewal property of HSPCs,[21] qRT-PCR analysis was conducted. The expression level of *GAPDH* in all samples was not significantly difference. The results showed that MSCs cultured on Scaffold-II have significantly higher expression of *JAG1* gene, compared to Scaffold-I (Fig. 2), suggesting that fibrous scaffolds with anisotropic properties are capable to induce haematopoiesis supportive function in MSCs that can facilitate successful *in vitro* expansion and retention of HSPCs potential to differentiate into various lineages.

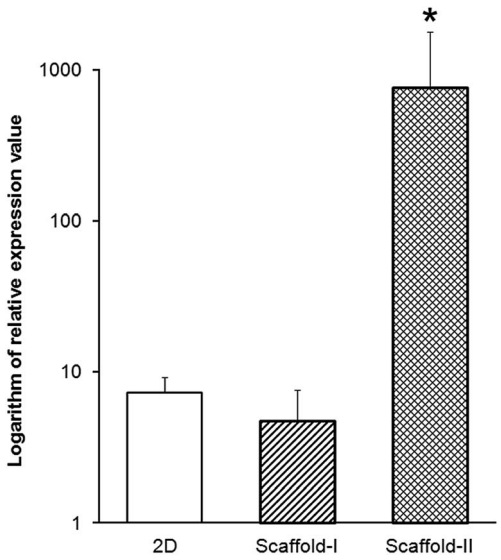


Fig. 2 *JAG1* expression in MSCs cultured on artificial niches. An asterisks represents significant difference (*$p < 0.05$).

### Expansion of hematopoietic stem/progenitor cells by using layered fiber scaffolds

The *in vitro* expansion efficiency of HSPCs in our 3D biohybrid hematopoietic niche was studied in comparison to the cells cultured in a conventional 2D system. The proliferation activity and immunophenotype of expanded HSPCs were analyzed by CD34 and CD38 double staining and FACS analysis after 7 days of culture; where CD34 is a classical HSPCs marker,[25] and $CD34^+CD38^-$ cells are primitive population of HSPCs.[13] The quantitative analysis of expanded HSPCs showed no significant difference among three groups. However, absolute cell number in both artificial niches was higher than in 2D control culture. Specifically, in 3D-I culture, $3.3 \times 10^5$ cells per $cm^2$ were counted, in 3D-II culture $3.5 \times 10^5$ cells per $cm^2$, and in 2D culture $1.8 \times 10^5$ cells per $cm^2$ (Fig. 3A). No significant difference was observed among these culture conditions in cell numbers.

Next, the cell population composition of each culture revealed that HSPCs cultured in 3D artificial niches retained their high CD34 expression compared to 2D culture. $CD34^+$ cell

Table 1 Parameters of obtained scaffolds

| | Scaffold geometry | Second-order parameter, $S$ | Fiber diameter (μm) | Pore size ($\mu m^2$) |
|---|---|---|---|---|
| Scaffold-I | Transversely isotropic | 0.96 ± 0.02 | 1.72 ± 0.52 | 32.8 ± 43.6 |
| Scaffold-II | Anisotropic | 0.51 ± 0.09 | 1.85 ± 0.5 | 8.6 ± 5.5 |

 This journal is © The Royal Society of Chemistry 2015

Published on 16 September 2015. Downloaded by Michigan State University on 28/01/2016 09:27:12.

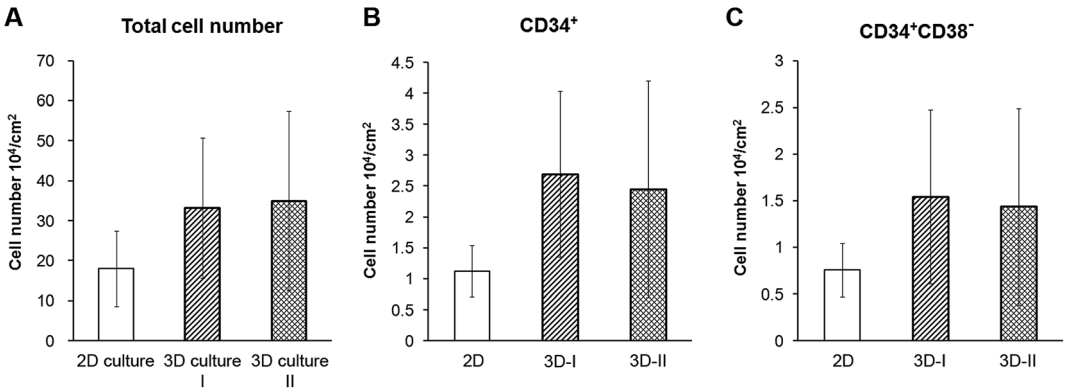


Fig. 3 (A) Quantification of total cell number in different culture conditions after 7 day coculture. (B) Total number of $CD34^+$ cells, (C) total number of $CD34^+CD38^-$ cells. Mean ± SD ($n = 3$).

population in 3D-I culture was $2.7 \times 10^4$ cells per $cm^2$, in 3D-II culture $2.5 \times 10^4$ cells per $cm^2$, and only $1.1 \times 10^4$ cells per $cm^2$ were quantified in 2D culture (Fig. 3B). The retention of primitive $CD34^+CD38^-$ phenotype analysis also showed that cells cultured in 3D artificial niches maintained the large number of $CD34^+CD38^-$ cells (Fig. 4), 3D-I = $1.5 \times 10^4$ cells per $cm^2$ and 3D-II = $1.4 \times 10^4$ cells per $cm^2$, after 7 days of culture. 3D cultures showed the tendency of higher number of $CD34^+CD38^-$ cells than 2D culture, however no significant difference was observed between the two 3D cultures (Fig. 3C).

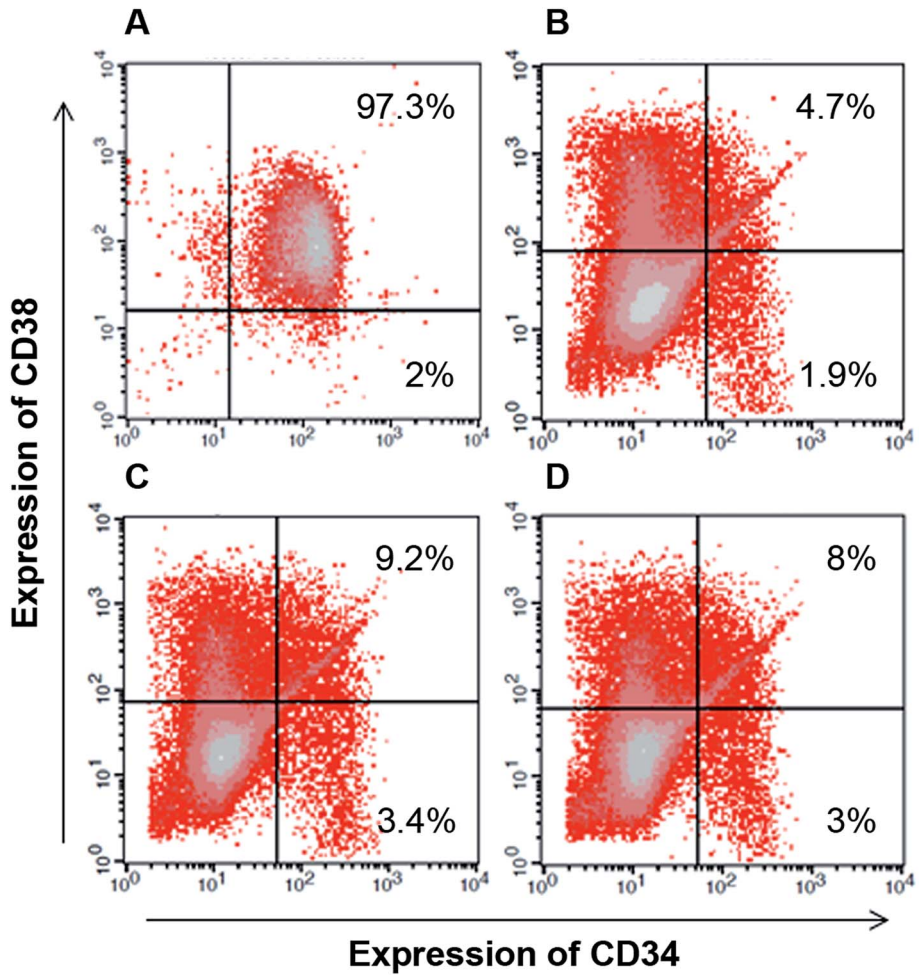


Fig. 4 CD34/CD38 expression in relation to the number of HSPCs after 7 day coculture. (A) $CD34^+$ cell fraction before coculture, (B) expanded cells cultured in 2D culture system, (C) in 3D culture-I and (D) in 3D culture-II.

Published on 16 September 2015. Downloaded by Michigan State University on 28/01/2016 09:27:12.

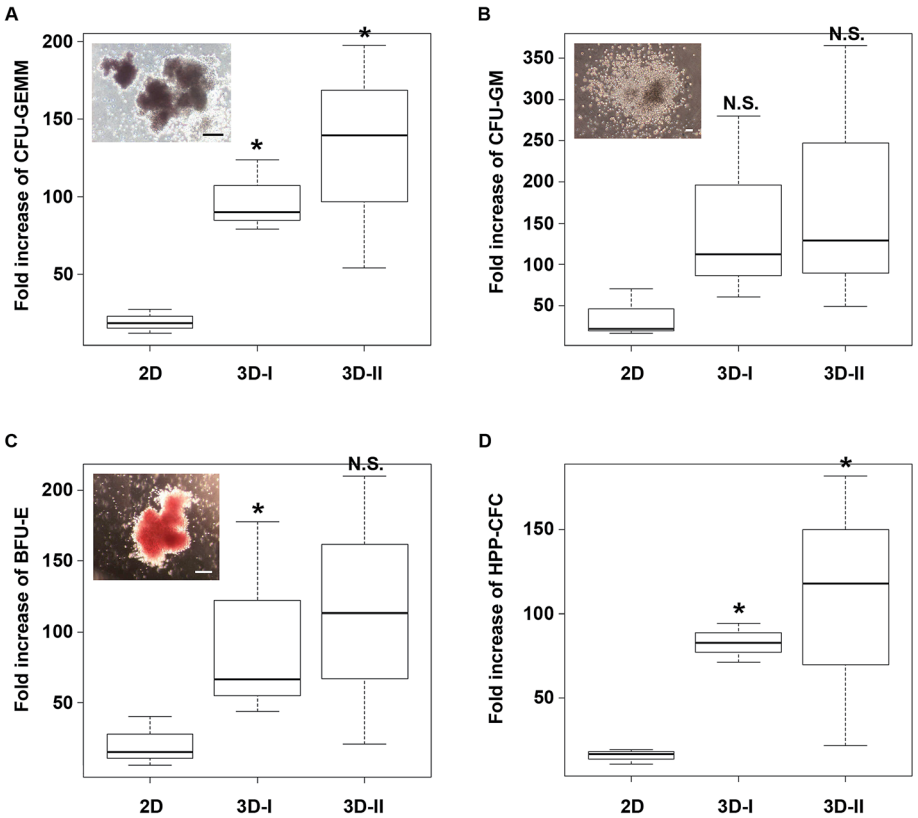


Fig. 5 Hematopoietic potency of the CD34$^+$ cell progeny after 14 days of culture in different culture systems represented in cell fold increase against cell number before culture. (A) CFU-GEMM (granulocytes/erythroid cells/macrophages/megakaryocytes), (B) CFU-GM (colony-forming unit-granulocyte/macrophages), (C) BFU-E (burst-forming unit-erythroids), (D) HPP-CFC (high-proliferative potential colony-forming cells) after 28 days culture. The box plot represents the maximum, the median and the minimum of values ($n = 3$). An asterisks represents significant difference from the control 2D culture (*$p < 0.1$). Insets are representative colony images (scale bars 100 μm).

### Hematopoietic functions of CD34$^+$ progeny cells

Hematopoietic potency of the CD34$^+$ progeny cells cultured in geometrically different 3D biohybrid niches was examined by CFU assay and compared with 2D culture. Expanded cells were examined for availability of CFU-GM, BFU-E, HPP-CFC and CFU-GEMM, where HPP-CFC and CFU-GEMM are multipotential progenitors and believed to be more primitive than the lineage-restricted CFU-GM and BFU-E. Morphology of obtained colonies is shown in insets of Fig. 5. CFU assay results showed that HSPCs expanded in 2D culture, 3D-I and 3D-II cultures with $10^3$ input cells gave rise to 2.7, 6.2, and 9.7 CFU-GEMM colonies; 3.9, 8.5, and 10 CFU-GM colonies; 3.7, 8.6, and 11.0 BFU-E colonies; respectively after 14 days of culture. After 28 days of culture 5.0, 12.7, and 16.7 HPP-CFC colonies were counted (Fig. S1†). The number of CFU-GEMM and HPP-CFC colonies in 3D-I culture was significantly higher than in the 2D culture indicating that our artificial hematopoietic niche is potential for maintaining multipotential properties of HSPCs. The comparison of fold change of initial cell number in 2D and 3D cultures shown in Fig. 5 revealed significant difference between these two culture systems except in formation of CFU-GM. As expected, 3D-II culture showed significantly high fold-increase in more primitive CFU-GEMM and HPP-CFC. These results show that 3D cultures are able to support proliferation of HSPCs, maintain their primitive phenotype, and accommodate large number of cells in comparison to the 2D culture, suggesting that the designed artificial niches have potential to be used as an *in vitro* expansion system for HSPCs that can fulfill the clinical necessity and quality of transplant HSPCs.

## Discussion

Due to the necessity for an improvement in the clinical outcome of HSPCs transplantation, the *in vitro* expansion of these cells is needed. In the 3D cultivation method of HSPCs, geometry and porosity of the scaffold are important regulatory, for the cell infiltration as well as for a distribution of soluble factors.[26] In this context, it was desired to mimic the bone endosteal microenvironment of BM, where HSPCs are nurtured.[15,27] To achieve this goal, we proposed a fabrication of 3D biohybrid hematopoietic niche composed of electrospun fiber scaffolds and MSCs as a feeder cells. Efficiency of the designed 3D biohybrid niche was compared with a conventional 2D culture system. In addition, in order to study the effect geometrical properties of the niche on proliferation capacity and functionality of expanded HSPCs, the niche composing fiber scaffolds were prepared with distinctive transversely isotropic or anisotropic properties.

 This journal is © The Royal Society of Chemistry 2015

Published on 16 September 2015. Downloaded by Michigan State University on 28/01/2016 09:27:12.

The first advantage of our electrospun fiber scaffolds is their microscale architecture with high surface-to-volume ratio and capacity to selectively enhance adsorption of ECM proteins that are able to modulate interactions of the cells with the environment and cell communication.[28] In the experimental results, HSPCs cultured in 3D biohybrid niche had higher proliferative potential and multipotency than that of 2D culture system. It appears that interconnected pores and micro-topography of each layer that consisted 3D biohybrid niche resembled the natural ECM facilitating formation and maturation of stronger cell focal adhesion and actin polymerization, which are important in MSCs osteogenesis.[29] Our previous study revealed that the same scaffolds with transversely isotropic and anisotropic properties can serve as a physical cue for controlling MSCs fate. MSCs seeded onto anisotropic fiber scaffolds committed to an osteogenic differentiation and were potential to deposit large amounts of calcium[22] that are essential for hematopoietic niche composing feeder cells.[21] Further coculture and methylcellulose-based CFU assay revealed superior potential of 3D biohybrid niches to give rise of higher number of colonies compared to 2D culture system. In case of 3D cultures, cells of 3D-II retained their highest potential to differentiate into multilineage progenitor cells and gave rise of higher number of colonies. Probably, microstructure of Scaffold-II of 3D-II culture more closely resembled the natural ECM as well as significantly high expression of *JAG1* in the feeder cells, which an important feature of HSPCs supporting cells,[13] might caused the obtained results. Since, the interaction between Notch-1 in HSPCs and Notch-1 ligand *JAG1* in stromal cells plays an important role in the self-renewal of HSPCs and retention of more primitive immunophenotype.[21,30] These results are also associated with location of HSPCs, according to Jing D *et al.*, in conventional 2D coculture system HSPCs, which had a direct contact with MSCs, had the highest proliferation capacity; however cells which migrated beneath MSCs monolayer had more primitive cells.[14] However, in our results, we have observed remarkable difference between two 3D cultures (Fig. 2), but the difference in cell increase was insignificant. This can be attributed to the effect of soluble factors. It is possible that interconnected pores of each fiber layer of the scaffold and the space (~200 μm) in-between fiber layers facilitated the formation of niche-like microenvironment allowing specific distribution of soluble factors as well as MSCs and HSPCs. That is, HSPCs that came into direct contact with MSCs might be stimulated into high proliferation state, and due to their small cell size, they migrated into the second and third layers of MSCs, which might consequently trigger further proliferation. Meanwhile, the non-adherent HSPCs that existed in-between the fiber layers might maintain their primitive phenotype (Fig. 6). Therefore, increasing the number of overlaid scaffolds might improve the efficiency of these culture systems.

These results suggest that the structural advancement of our 3D biohybrid niche is capable of facilitating high-density expansion of multipotent HSPCs.

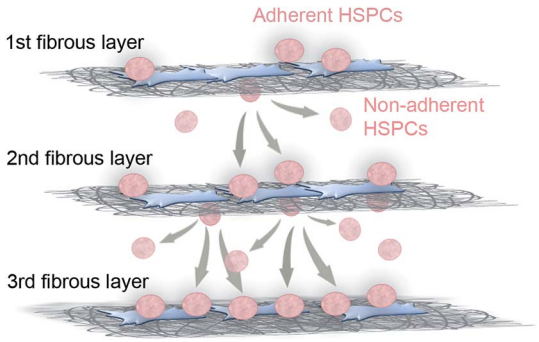


Fig. 6 Proposed mechanism of the retention of HSPCs proliferative and primitive phenotype in 3D beehive-like biohydrid niche.

The second important aspect of our 3D niche is its mechanical property. Compared to 2D culture system, cells cultured in 3D-I cultures had 2-fold higher number of primitive cells such as CFU-GEMM and HPP-CFCs (Fig. S1†). The 3D-II culture showed no significant difference due to the effect of cord blood lots, but had similar tendency to 3D-I. Like BM niche, our 3D biohybrid niches regulate the mechanotransduction of HSPCs, where the involvement of actin–myosin cytoskeleton and membrane receptors such as integrins help them to sense their microenvironment.[31] Recent study showed that substrate elasticity promotes two- to three fold expansion of HSPCs, probably resembling certain diseased state of the tissue.[32] Thus we consider that elasticity of our scaffolds also promoted the expansion of HSPCs.

The third important aspect of our 3D niche is its beehive-like structure that is easy to assemble and disassemble allowing efficient collection of cultured cells from each scaffold layer. In the assembled scaffold the distance between fiber scaffold layers allows sufficient exchange of nutrition and oxygen as well as the removal of metabolic waste of the cells. Since, in this study 3D cell culture experiments were carried out in a small volume static medium, only three layers of fiber scaffolds were used in order to prevent oxygen depletion. Size and structural modifications of our artificial niche can be done upon necessity to obtain higher than $1.7 \times 10^5$ $CD34^+$ cells per kg to facilitate high survival of the patient.[33]

## Conclusions

In this study, we fabricated 3D biohybrid hematopoietic niches for the expansion of clinically important HSPCs. Compared to the conventional 2D culture system our designed 3D biohybrid niches can facilitate niche-like microenvironment to support proliferation activity and retention of primitive phenotype in HSPCs. 3D biohybrid niche consisting scaffolds were able to control chemical signals secretion from feeder MSCs through mechanotransduction to facilitate successful *in vitro* expansion and retention of HSPCs with superior potential to differentiate into various lineages.

Published on 16 September 2015. Downloaded by Michigan State University on 28/01/2016 09:27:12.

Future work will be focused on the development of more effective 3D biohybrid niches with higher number of fibrous layers and applicable for microscopy observations.

## Conflict of interest

The authors declare no competing financial interest.

## Acknowledgements

This research was partially supported by JSPS KAKENHI Grant Number 25870272 and JST A-STEP No. AS251Z02503P.

## References

1 S. Méndez-Ferrer, T. V. Michurina, F. Ferraro, A. R. Mazloom, B. D. MacArthur, S. A. Lira, D. T. Scadden, A. Ma'ayan, G. N. Enikolopov and P. S. Frenette, *Nature*, 2010, **466**, 829–834.
2 M. Remberger, J. Mattsson, R. Olsson and O. Ringdén, *Clin. Transplant.*, 2011, **25**, E68–E76.
3 E. A. Copelan, *N. Engl. J. Med.*, 2006, **354**, 1813–1826.
4 A. Mendelson and P. S. Frenette, *Nat. Med.*, 2014, **20**, 833–846.
5 Y. Xie, T. Yin, W. Wiegraebe, X. C. He, D. Miller, D. Stark, K. Perko, R. Alexander, J. Schwartz and J. C. Grindley, *Nature*, 2008, **457**, 97–101.
6 N. J. Chao, S. G. Emerson and K. I. Weinberg, *ASH Education Program Book*, 2004, vol. 2004, pp. 354–371.
7 M. J. Laughlin, M. Eapen, P. Rubinstein, J. E. Wagner, M.-J. Zhang, R. E. Champlin, C. Stevens, J. N. Barker, R. P. Gale and H. M. Lazarus, *N. Engl. J. Med.*, 2004, **351**, 2265–2275.
8 S. Agrawal, P. Tripathi and S. Naik, *Nova Book*, 2009, pp. 25–41.
9 M. Körbling and T. Fliedner, *Bone Marrow Transplant.*, 1996, **17**, 675–678.
10 P. Dhot, V. Nair, D. Swarup, D. Sirohi and P. Ganguli, *Indian J. Pediatr.*, 2003, **70**, 989–992.
11 K. Ohishi, B. Varnum-Finney and I. D. Bernstein, *J. Clin. Invest.*, 2002, **110**, 1165–1174.
12 V. M. Sandler, R. Lis, Y. Liu, A. Kedem, D. James, O. Elemento, J. M. Butler, J. M. Scandura and S. Rafii, *Nature*, 2014, **511**, 312–318.
13 T. Walenda, S. Bork, P. Horn, F. Wein, R. Saffrich, A. Diehlmann, V. Eckstein, A. D. Ho and W. Wagner, *J. Cell. Mol. Med.*, 2010, **14**, 337–350.
14 D. Jing, A. V. Fonseca, N. Alakel, F. A. Fierro, K. Muller, M. Bornhauser, G. Ehninger, D. Corbeil and R. Ordemann, *Haematologica*, 2010, **95**, 542–550.
15 B. Guezguez, C. J. Campbell, A. L. Boyd, F. Karanu, F. L. Casado, C. Di Cresce, T. J. Collins, Z. Shapovalova, A. Xenocostas and M. Bhatia, *Cell Stem Cell*, 2013, **13**, 175–189.
16 L. Wang, R. Benedito, M. G. Bixel, D. Zeuschner, M. Stehling, L. Sävendahl, J. J. Haigh, H. Snippert, H. Clevers and G. Breier, *EMBO J.*, 2013, **32**, 219–230.
17 K. N. Chua, C. Chai, P. C. Lee, S. Ramakrishna, K. W. Leong and H. Q. Mao, *Exp. Hematol.*, 2007, **35**, 771–781.
18 M. Kucia, J. Ratajczak and M. Z. Ratajczak, *Exp. Hematol.*, 2005, **33**, 613–623.
19 R. D. Nandoe Tewarie, A. Hurtado, A. Levi and J. A. Grotenhuis, *Cell Transplant.*, 2006, **15**, 563–577.
20 T. Okamoto, T. Aoyama, T. Nakayama, T. Nakamata, T. Hosaka, K. Nishijo, T. Nakamura, T. Kiyono and J. Toguchida, *Biochem. Biophys. Res. Commun.*, 2002, **295**, 354–361.
21 S. Fujita, J. Toguchida, Y. Morita and H. Iwata, *Cell Transplant.*, 2008, **17**, 1169–1179.
22 S. Fujita, H. Shimizu and S. Suye, *J. Nanotechnol.*, 2012, **2012**, 429890.
23 R. S. Stein and F. H. Norris, *J. Polym. Sci.*, 1956, **21**, 381–396.
24 S. Nomura, H. Kawai, I. Kimura and M. Kagiyama, *J. Polym. Sci., Polym. Phys. Ed.*, 1970, **8**, 383–400.
25 S. Kanji, M. Das, R. Aggarwal, J. Lu, M. Joseph, S. Basu, V. J. Pompili and H. Das, *Stem Cell Res.*, 2014, **12**, 275–288.
26 A. Raic, L. Rödling, H. Kalbacher and C. Lee-Thedieck, *Biomaterials*, 2014, **35**, 929–940.
27 M. Hines, L. Nielsen and J. Cooper-White, *J. Chem. Technol. Biotechnol.*, 2008, **83**, 421–443.
28 X. Liu and P. X. Ma, *Ann. Biomed. Eng.*, 2004, **32**, 477–486.
29 C. H. Seo, H. Jeong, Y. Feng, K. Montagne, T. Ushida, Y. Suzuki and K. S. Furukawa, *Biomaterials*, 2014, **35**, 2245–2252.
30 L. Calvi, G. Adams, K. Weibrecht, J. Weber, D. Olson, M. Knight, R. Martin, E. Schipani, P. Divieti and F. Bringhurst, *Nature*, 2003, **425**, 841–846.
31 C. Huang and R. Ogawa, *FASEB J.*, 2010, **24**, 3625–3632.
32 J. Holst, S. Watson, M. S. Lord, S. S. Eamegdool, D. V. Bax, L. B. Nivison-Smith, A. Kondyurin, L. Ma, A. F. Oberhauser and A. S. Weiss, *Nat. Biotechnol.*, 2010, **28**, 1123–1128.
33 J. E. Wagner, J. N. Barker, T. E. DeFor, K. S. Baker, B. R. Blazar, C. Eide, A. Goldman, J. Kersey, W. Krivit and M. L. MacMillan, *Blood*, 2002, **100**, 1611–1618.

 This journal is © The Royal Society of Chemistry 2015